Thermal Expansion Behavior of Al/Magnesia Metal Matrix Composites

Chennakesava R Alavala

Department of Mechanical Engineering, JNT University, Hyderabad, India

Abstract: *The coefficient of thermal expansion (CTE) of aluminum matrix composites having different volume fractions of MgO particulate have been investigated. The composites were produced powder metallurgy technique by mixing and packing MgO nanoparticles of 100 nm. The experimental results for composites indicate negligible hysteresis in the CTE curves during heating and cooling cycles. Comparison is made between the experimental data and several model predictions. Among the model predictions, the Kerner, Turner and Scahpery models offer the highest values. Turner's equation gave the best correlation between mechanical and thermal-expansion characteristics of the composites. All the other equations can be used as well, because the coefficient of correlation is over 90 %.*

Keywords: Metal matrix composites, magnesia, thermal expansion, theoretical models.

1. Introduction

Metal matrix composites have been used as a structural material for high temperature applications such as engine components [1] and gas turbines. Metal matrix composites have excellent physical and mechanical properties compared with unreinforced monolithic alloys [2-5]. Many researchers have stated that the mismatch of coefficient of thermal expansion (CTE) between particulate and matrix was mostly attributable for the degradation of composites subjected to thermal cycling [2]. In general the matrix CTE was much larger than that of the reinforcing particulate. Hence, internal stresses arise in the composite as the temperature changes. Changes in internal stresses cause residual dimensional changes of the composite specimens [6-11]. Many theoretical models such as Turner's Schapery's and Kerner's have been developed to predict thermal expansion of metal matrix composites [12-14].

The simplest equation to estimate the thermal expansion of two-phase materials is the rule of mixtures (ROM), Eq. (1). Turner took the elastic constant into account in CTE equation, Eq. (2). The spherical shape of the second phase is considered by Kerner, Eq. (3), and Schapery, Eq. (4) and (5). The upper and lower bounds for elastic modulus have been well established by Schapery.

$$\alpha_c = \alpha_r V_r + \alpha_m V_m \tag{1}$$

$$\alpha_c = \frac{\alpha_m V_m K_m + \alpha_r V_r K_r}{V_m K_m + V_r K_r} \tag{2}$$

$$\alpha_c = \alpha_m V_m + \alpha_r V_r + V_m V_r (\alpha_r - \alpha_m)\frac{K_r - K_m}{V_m K_m + V_r K_r + 3K_m K_r/4G_m} \tag{3}$$

$$\alpha_c = \alpha_m V_m + \alpha_r V_r + \frac{4G_m}{K_c}\frac{(K_c - K_r)(\alpha_m - \alpha_r)V_r}{4G_m + 3K_r} \tag{4}$$

$$\alpha_c = \alpha_m V_m + \alpha_r V_r + \frac{4G_r}{K_c}\frac{(K_c - K_m)(\alpha_r - \alpha_m)V_m}{4G_m + 3K_m} \tag{5}$$

where α is CTE, V the volume fraction, K the bulk modulus, G shear modulus and the subscripts c, m, and r refer to the composite, matrix and reinforcement, respectively.

The modeling and numerical computation have explored to compute thermal expansion of aluminum matrix composite with densely packed SiC particles [15]. The physical CTE of aluminum matrix composite reinforced with 70% volume fraction of SiC particles has been analytically computed to explicate the deviations in the thermal expansion behavior obtained experimentally. The thermal expansion behavior of a composite is governed by several material parameters, such as, the volume fraction of constituents, the microstructure of constituents, the presence of voids and the mismatch of CTE of constituents [16].

The characterization and analysis of thermal properties viz., thermal conductivity, thermal diffusivity, thermal shock resistance, thermal expansion and specific heat capacity are advantageous for aerospace and automotive applications, electronic packaging and thermal management equipment. The aim of this paper was to predict the thermal expansion behavior of aluminum metal matrix composites reinforced with nanoscale magnesia (MgO) particles. The effect of volume fraction of MgO nanoparticles was also examined.

Table 1: Composition of metal matrix composites

Composite	Composition, vol.%	
	Al	MgO
AL-MGO-1	90	10
AL-MGO-2	85	15
AL-MGO-3	80	20
AL-MGO-4	75	25

2. Materials and Methods

Pure Al powder of 100 μm with 99.9% purity and MgO powders of 100 nm were used as the starting materials. Pure powders of Al and MgO, in the desired volume fractions, were mixed together by high-energy ball milling for 20 h to ensure the uniform mixing. The mixing was carried out in argon atmosphere to minimize the contamination. The

obtained powder mixtures were then sintered to bulk specimens by hot pressing at 800 °C with a pressure of 50 MPa in vacuum, followed by quickly cooling to room temperature in 30 min. In this study, four different composites were prepared (Table 1).

The thermal expansion was then measured with a dilatometer (DIL 802) between 100 and 300°C at heating and cooling rates of 5°C/min in argon. With this instrument the difference in length between the specimen to be investigated and a reference sample is measured, which results in a resolution of ± 0.01 μm. The sample holder (pushrod) is made of sapphire (figure 1). Specimens with a diameter of 5 mm and length of 10 mm were used for CTE measurement. The instantaneous CTE at a given temperature was calculated using the following equation:

$$\text{CTE} = \frac{\partial}{\partial T}\left(\frac{\Delta L}{L}\right) \qquad (6)$$

where L is the length of the specimen and T the temperature.
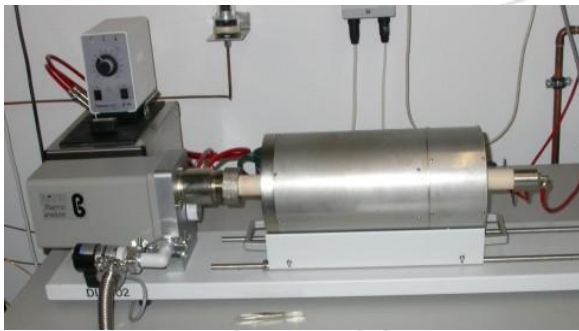

Figure 1: The differential dilatometer.

3. Results and Discussion

The microstructure studies revealed a uniform distribution of MgO nanoparticles with meager micro-segregation of nanoparticles in the composites made from mixtures. Representative microstructures of composites made from mixtures containing 10%, 15%, 20% and 25% of nanoparticles are shown in figure 2. The MgO particles are slightly elongated in a direction perpendicular to the hot-pressing direction.
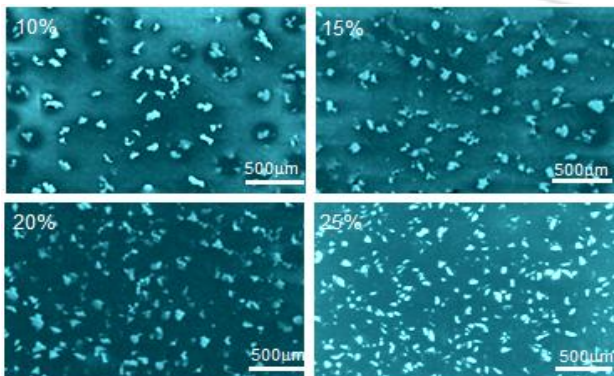

Figure 2: Optical micrographs of composites made from nanoparticle mixture containing 10% (a), 15% (b), 20% (c) and 25% (d).
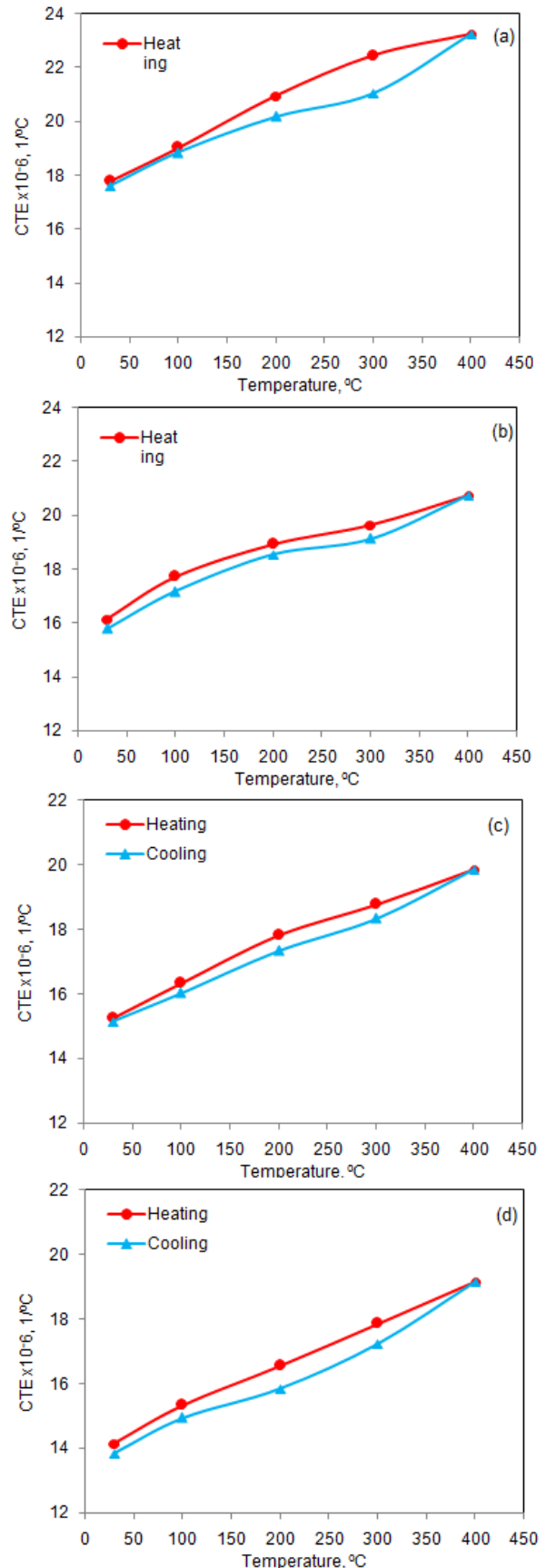

Figure 3: Coefficient of thermal expansion as a function of temperature for: (a) AL-MGO-1, (b) AL-MGO-2, (c) AL-MGO-3 and (d) AL-MGO-4.

The CTE obtained from the heating and cooling as a function of temperature is plotted in figure 3 for all composites. The

CTE measured during the heating cycle increases nonlinearly for the composites with increasing temperature between 30 and 400°C as shown in figure 3. The results shown in Fig. 3 clearly indicate that the thermal expansion is not linearly related with temperature. The CTE measured during the cooling cycle decreases continuously with decreasing temperature in the same trend of heating cycle. The Δt is used to quantify the hysteresis in the curve and is the largest vertical (at a given temperature) difference between the cooling and heating curves. It is noted that the hysteresis gradually decreases as the temperature decreases. Negligence of the hysteresis effect proves that all these systems are in a thermal equilibrium.

Figure 4 compares the thermal expansion behavior of the four samples obtained from the heating cycle. It can be seen that the CTE value decreases with increase in volume fraction of MgO nanoparticles. The bond energy is low for the composites having high volume fraction of MgO nanoparticles. The strong dependence of the CTE on particle volume fraction can be qualitatively understood by taking account of the CTE mismatch between Al and MgO. The significantly smaller CTE of the ceramic, as compared to that of Al, explains why it sharply decreases with volume fraction of MgO. For the composite materials, residual stresses resulted from thermal mismatch between the matrix and the reinforcement influences the thermal expansion behavior.
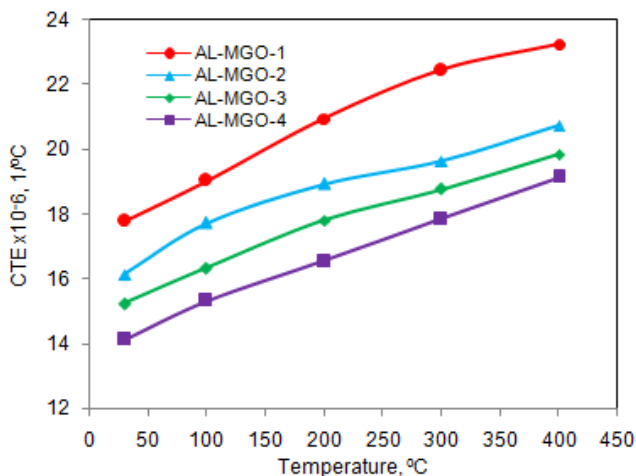

Figure 4: Compare the CTE of different composites

Several equations have been proposed for predicting the thermal expansion coefficient in dependence on the thermal and elastic properties of the constituents and the volume fraction of each phase. The simplest approach is the linear rule of mixtures (ROM). If the included phase has spherical geometry, the most popular equations are those given by: Turner [12], Kerner [13], and Schapery [14]. These models were used to calculate the CTE of the materials investigated here. Figure 5 compares the experimental results with the theoretical models for all four composites. A comparison of experimental results with those obtained using the model equations lead to the conclusion that Turner's equation gives the best correlation between mechanical and thermal-expansion characteristics, but it is obvious that all the other equations can be used as well, because the coefficient of correlation is over 90 %. It may be concluded that the range of particle volume fraction over which the data lie in between

Schapery's bounds becomes narrower as the temperature is increased.
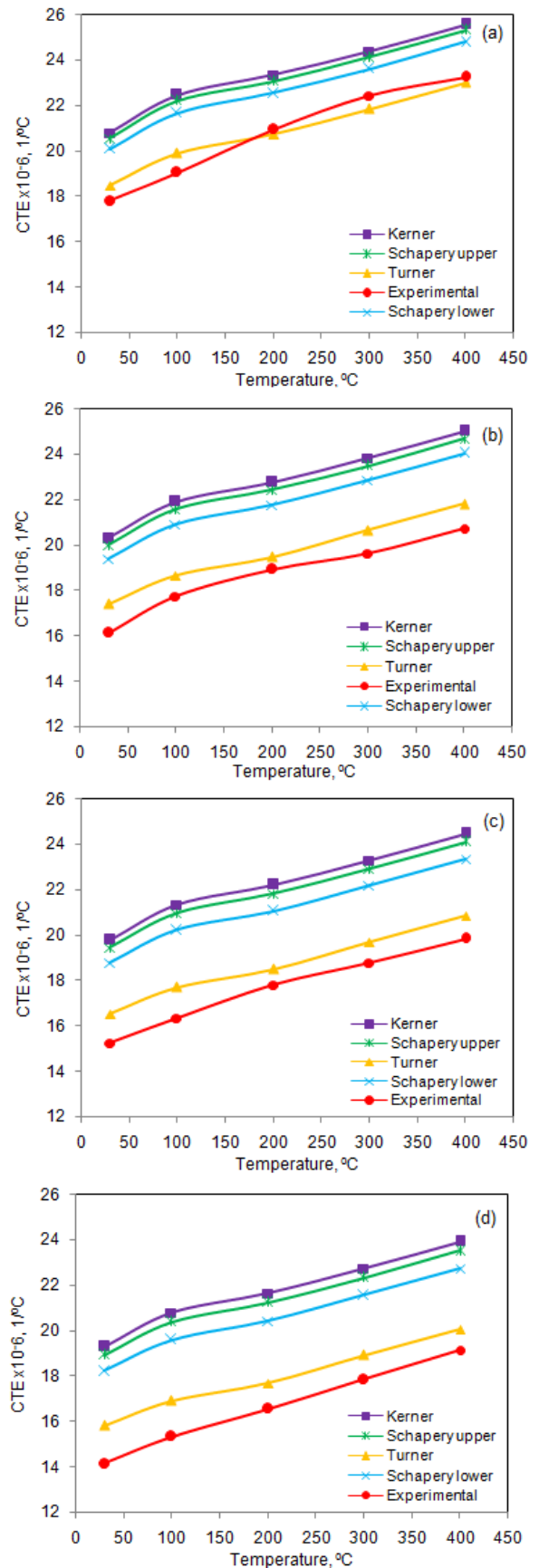

Figure 5: Coefficient of thermal expansion as a function of temperature compared with Schapery and Turner models for: (a) AL-TB-1, (b) AL-TB-2, (c) AL-TB-3 and (d) AL-TB-4.

Paper ID: ART20161293 1819

The large difference between the coefficients of thermal expansion of the aluminum and the MgO particles induces stresses and increases the dislocation density in the metal. As a result, the metal is hardened up to an extent that is greater the higher is the reinforcement content. As the previous models do not take into account this hardening, one may expect the predicted variation of the CTE with particle volume fraction to be lower than observed experimentally.

Magnesia (MgO) is a white hygroscopic solid. It has an empirical formula of MgO and consists of a lattice of Mg^{2+} ions and O^{2-} ions held together by ionic bonding. The crystal structure as shown in figure 6 resembles the rock salt crystal structure.
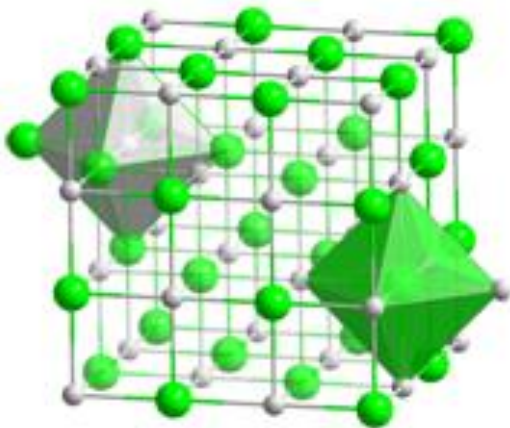

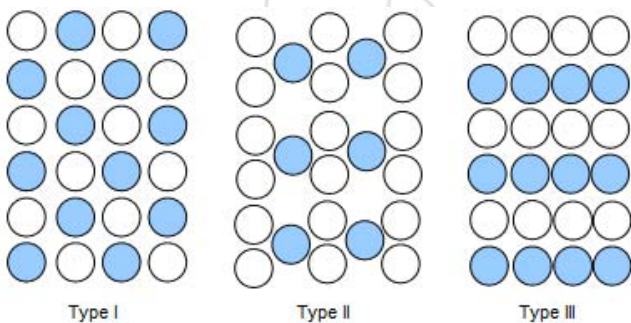**Figure 6:** Halite (cubic) crystal structure of MgO

Figure 7: Stability of oxide surface

Single crystal MgO exhibits cubic symmetry as shown in figure 6. The lattice parameters have a slight quadratic dependence on the temperature which accounts for the linear temperature dependence of the coefficient of thermal expansion. Tasker [17] proposed a classification of oxide surfaces based purely on electrostatic criteria. In this model, the crystal is represented by a stack of planes perpendicular to the surface. The planes are arranged in a way to give an electrostatic neutral building block, which builds up the whole crystal as shown in figure 7. The surfaces are classified by the net charge Q in a plane and the dipole moment μ of the building block perpendicular to the surface. Polar surface (Type III) of MgO (111) is unstable due to the diverging electrostatic energy caused by the finite dipole moment in all building blocks. These surfaces are unstable and due to either structural or electronic modification. The image of the MgO surface shown in figure 8 has been obtained by noncontact atomic force microscopy (AFM) [18]. Large (100) terraces are exposed that are separated by

monoatomic steps. For MgO, the chemical nature of the sublattice cannot be identified on the basis of the AFM results presented. MgO (100) has neutral layers and it is non-polar; wheras MgO (111) has charged layers and it is polar.
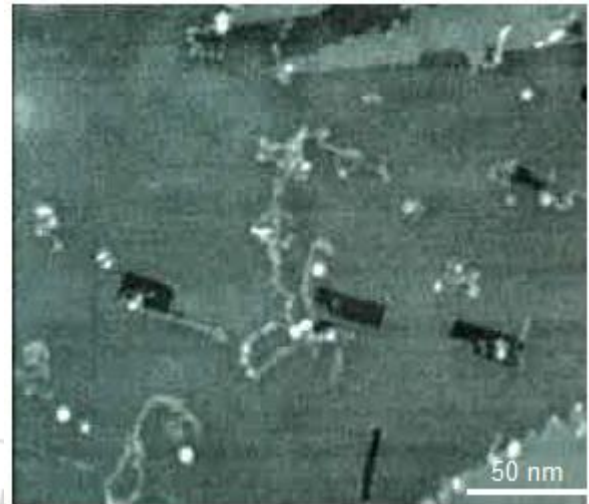

Figure 8: Large-scale and atomically resolved AFM images of the surface of MgO (100) single crystal; from Barth [18].
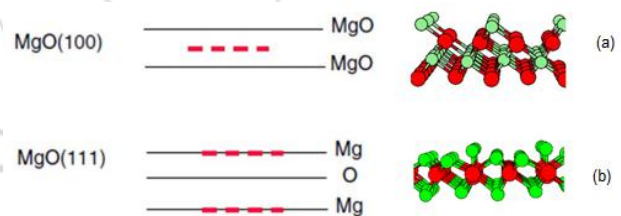

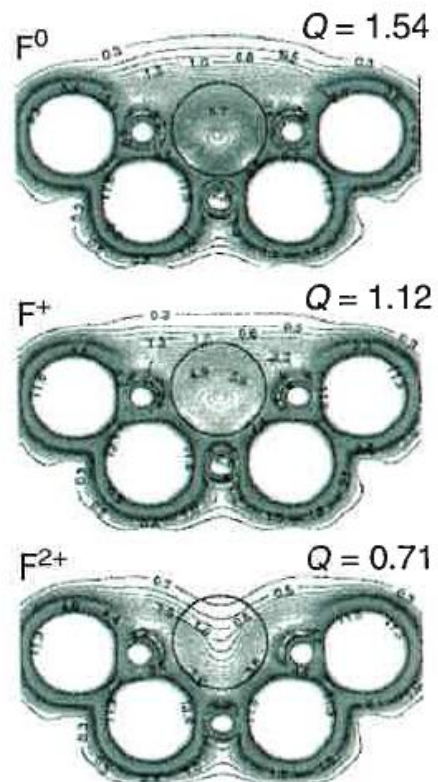**Figure 9:** Polar status of MgO.

Figure 9: Electron density plots for the three charge states of oxygen vacancies on the MgO surface from Sushko [19].

On the MgO surface, oxygen vacancies can occur in three different charge states. A bare vacancy, is obtained by removal of an O^{2-} ion. Oxygen vacancies occupied by either one or two electrons are called F+ and F^0 centers, respectively. It has been suggested for a long time that F centers exist on the surface of MgO. In figure 9, electron density plots for the three charge states of the anion vacancy on the (100) surface of MgO are shown, together with values of the electron density Q integrated within the spheres depicted in the images.

4. Conclusions

In this research, the thermal expansion behavior of Al-based composites reinforced with magnesia nanoparticles has been investigated. The coefficient of thermal expansion calculated over a wide temperature range (50–400°C) turns out to decrease linearly with the particle volume fraction. The results show that the CTE varies with temperature at a swiftness that is higher for pure aluminum than for the composites, a direct consequence of CTE characteristic of MgO. All composite types were in thermal equilibrium with negligible hysteresis effect. Turner's equation gave the best correlation between mechanical and thermal-expansion characteristics of the composites.

References

[1] A. C. Reddy, B. Kotiveerchari and P. Rami Reddy, Saving of Thermal Energy in Air-Gap Insulated Pistons Using Different Composite Materials for Crowns, International Journal of Scientific & Engineering Research, 6 (3), 71-74, 2015.

[2] A. C. Reddy, Influence of strain rate and temperature on superplastic behavior of sinter forged Al6061/SiC metal matrix composites, International Journal of Engineering Research & Technology, 4 (2), 189-198, 2011.

[3] A. C. Reddy, Evaluation of mechanical behavior of Al-alloy/SiC metal matrix composites with respect to their constituents using Taguchi techniques, i-manager's Journal of Mechanical Engineering, 1(2), 31-41, 2011.

[4] A. C. Reddy, Estimation of Thermoelastic Behavior of Three-phase: AA1100/Ni-Coated Boron Carbide Nanoparticle Metal Matrix Composites, International Journal of Scientific & Engineering Research, 6 (10), 662-667, 2015.

[5] A. C. Reddy, Evaluation of mechanical behavior of Al-alloy/Al2O3 metal matrix composites with respect to their constituents using Taguchi, International Journal of Emerging Technologies and Applications in Engineering Technology and Sciences, 4 (2), 26-30, 2011.

[6] Taya, Minoru, R.J. Arsenault. Metal Matrix Composites; Thermomechanical behaviour. Pergamon Press, 1989.

[7] A. C. Reddy, Simulation of MgO/AA6061 Particulate-Reinforced Composites Taking Account of CTE Mismatch Effects and Interphase Separation, In the Proceedings of the 3rd National Conference on Materials and Manufacturing Processes, Hyderabad, India, 22-25 February 2002, pp. 184-187.

[8] A. C. Reddy, Thermal Expansion Studies on Aluminum Matrix Composites with Different Reinforcement Volume Fractions of Si_3N_4 Nanoparticles, In the Proceedings of the 4th International Conference on Composite Materials and Characterization, Hyderabad, 7-8 March 2003, pp. 221-225.

[9] A. C. Reddy, Prediction of CTE of Al/TiB2 Metal Matrix Composites, In the Proceedings of the 3rd International Conference on Composite Materials and Characterization, Chennai, 11-12 May 2001, pp. 270-275.

[10] A. C. Reddy, Evaluation of Thermal Expansion of Al/B4C Metal Matrix Composites, In Proceedings of the 3rd National Conference on Materials and Manufacturing Processes, Hyderabad, 22-25 February 2002, pp. 196-200.

[11] A. C. Reddy, Thermal Expansion Behavior of Aluminum Matrix Composites Reinforced with Fused Quartz Nanoparticles, In the Proceedings of the National Conference on Advanced Materials and Manufacturing Techniques, Hyderabad, 08-09th March 2004, pp. 350-355.

[12] P.S. Turner, Thermal Expansion Stresses in Reinforced Plastics, Journal of Research of the National Bureau of Standards, 37, 239-250, 1946.

[13] E.H. Kerner, The elastic and thermo-elastic properties of composite media, Proceedings of the Physical Society. 69, 808–813, 1956.

[14] R. A. Schapery, Thermal expansion coefficients of composite materials based on energy Principles, Journal of Composite Materials, 2, 380-404, 1968.

[15] T. H. Nam, G. Requena, H.P. Degischer, Modelling and Numerical Computation of Thermal Expansion of Aluminium Matrix Composite, Composites Part A, 259-267, 2007.

[16] T. Huber, H.P. Degischer, G. Lefranc, T. Schmitt, Thermal Expansion Studies on Aluminum-matrix Composites with Different Reinforcement Architecture of SiC Particles Composites Science and Technology Compos. Sci. Technol. 66, 2206–2217, 2006.

[17] P.W. Tasker, The stability of ionic crystal surfaces, Journal of Physics C: Solid State Physics, 12, 4977-4984.1979.

[18] C. Barth, C. R. Henry, Atomic resolution imaging of the (001) surface of UHV cleaved MgO By dynamic scanning microscopy, Phys. Rev. Lett. 91, 196102 (2003).

[19] P.V. Sushko, A.L. Shluger, R.A. Catlow, Relative energies of surface and defect states: ab initio calculations for the MgO (001) surface, Surface Science, 50 (3), 153-170, 2000.